

## Enhanced Corrosion Resistance of TA2 Titanium via Anodic Oxidation in Mixed Acid System

Jieqin Lu, Guoying Wei\*, Yundan Yu, Xuping Zhao, Yifan Dai

College of materials science and engineering, China Jiliang University, Hangzhou310018, China

\*E-mail: [15067135751@163.com](mailto:15067135751@163.com)

Received: 8 December 2016 / Accepted: 23 February 2017 / Published: 12 March 2017

Anodic oxidation has been successfully used for surface modification of the titanium alloys. TiO<sub>2</sub> layers formed by anodization were modified the structure, apatite-forming ability and corrosion resistance of TA2 titanium alloy, in tartaric-sulfuric-oxalic acid system. Effects of different anodizing voltages and duration on the microstructure and performances of titania surface were investigated for anodizing TA2 titanium. The results showed that the TA2 titanium surface was covered with porous anatase and rutile after anodization which the thickness of the oxide layer achieved about 500nm. The corrosion resistance has been largely improved because the corrosion current density ( $2.044 \times 10^{-5}$  A/cm<sup>2</sup> and  $2.725 \times 10^{-5}$  A/cm<sup>2</sup>) decreased a magnitude compared with untreated TA2 titanium ( $2.725 \times 10^{-4}$  A/cm<sup>2</sup>), when the TA2 titanium was anodized under the condition of 40V for 40 min. After soaking in SBF, apatite formed on the TiO<sub>2</sub> layers and it covered the most parts of the surface when anodized at 40V for 10 min. Also, the EDS results revealed that Ca/P of the apatite films which demonstrated that the TiO<sub>2</sub> layers were short of calcium compared to hydroxyapatite.

**Keywords:** apatite formation; corrosion resistance; TA2 titanium alloy; anodic oxidation

### 1. INTRODUCTION

As is well-known, titanium alloys with excellent corrosion resistance, biocompatibility, low elastic modulus and good mechanical properties[1-5], are largely used as metallic implants applied in orthopedic, dental and maxillofacial fields[6-8]. It was also known that if the implant was harmful to human body, it might cause inflammation and allergic reactions, that meant it was an unsuccessful implant [9]. The implant might also bring some released metal ions to the body which could as well result in allergic and poisonous reactions [10]. Therefore, the better biocompatibility and higher corrosion resistance of the implants should be required. Investigations showed that, amorphous TiO<sub>2</sub> layers on the titanium alloy displayed inferior biocompatibility than crystalline TiO<sub>2</sub>, which might

cause failure in implanting [11-13]. Piazza et al.[14] pointed out that the anodic oxide conditions (applied voltage, the used electrolyte and annealing) played an important role in determining the layer crystallinity, additionally, annealing could induce forming the anatase and rutile phase. Chung et al.[15] proposed that the anatase phase could lead to better biocompatibility and corrosion resistance, also studied the Ti $\rightarrow$ TiO $\rightarrow$ anatase via anodizing and annealing. In addition, the HAp films was a necessary candidate to measure the biocompatibility of the materials [16].

In view of the above problems, anodizing for titanium alloys is an effective surface treatment to improve the biocompatibility and corrosion resistance, which can also enhance the stability of the titanium implants by fabricating porous oxide layer on the surface of titanium alloys [17-25]. In the process of the anodic oxidation of titanium or titanium alloy, TiO<sub>2</sub> layer grew both on the substrate/oxide and on the oxide/solution at the same time. The thickness of TiO<sub>2</sub> layers grown on the substrate/oxide depended on the migration of titanium ions to oxide/solution interface through oxide layers; thus, the growth on the interface of the oxide and solution determined by the transportation of titanium ions to substrate/oxide interface [26].

By anodization, the titanium surface could be modified to achieve better performances. Yang et al.[27] studied that titanium alloys anodized in H<sub>2</sub>SO<sub>4</sub> solution with different concentrations, performed better apatite-forming abilities when soaked in SBF for 6d, which also showed that heat treatment could induce the apatite formation on the surface. Hsu et al.[28] investigated self-organized TiO<sub>2</sub> nanotubes fabricated in NH<sub>4</sub>F/NaCl electrolyte, using commercially pure titanium anodised at 5V or 10V. The study found that the thickness of the Ca-P layer increased as the anodized potential and the average thickness of the Ca-P layer on Ti anodized at 5V and 10V with the thickness of 170nm and 190nm when immersion in simulated body fluid for 14 days, respectively. Lee et al.[29]studied the corrosion resistance and biocompatibility of anodized titanium and found that the anodized titanium improved the bioactivity when the HA films were deposited on the surface of the anodized titanium to enhance the anticorrosion compared with untreated titanium. Yue et al.[30] studied the bioactive surfaces of titanium plates treated with anodic oxidation (AO-Ti), alkali-heat (AH-Ti) and acid-alkali (AA-Ti) methods and found that anodic oxidation was an effective method which could endow the surface bioactivity and antimicrobial property, consequently, in favour of increasing the successful rate of clinic implants. So far, the anodic oxidation for titanium alloys was applied as a good method to obtain some certain microstructures and improve the biocompatibility and corrosion resistance.

Our work aimed to prepare porous TiO<sub>2</sub> layer on the surface of the TA2 titanium alloys using anodic oxidation by changing the applied voltages and anodized durations from tartaric-sulfuric-oxalic acid system to obtain better anti-corrosion properties and biocompatibility. The apatite-forming ability by soaking in SBF[31] and corrosion resistance in Hank's solution were investigated.

## 2. EXPERIMENTAL

TA2 titanium alloy Samples were cut into 26×8×1mm. Before anodization, the TA2 surfaces were polished on metallographic emery paper with different granulations (from 600 to 2000 mesh);

After that, the samples were polished on the polisher to make the surfaces more bright and flat, then cleaned in acetone and deionized water.

The electrolyte consisted of tartaric acid, sulfuric acid and oxalic acid with different concentrations (Table 1). Pure titanium sheet was used as cathode and TA2 titanium alloy as anode; Anodizing of titanium alloys were anodized at different DC voltages (from 10V to 50V) for 20 min. Different anodized durations (from 10 min to 60 min) at 30V. The temperature was controled to 25 °C during the whole anodization. After the anodization, the samples were cleaned in deionized water and dried by hair dryer. Anodic oxidation experiment equipment was showed in Fig. 1.

**Table 1.** Composition of electrolyte (in 200mL deionized water)

Chemicals	Specifications	Content
C <sub>4</sub> H <sub>6</sub> O <sub>6</sub>	AR	7g
H <sub>2</sub> C <sub>2</sub> O <sub>4</sub>	AR	6g
H <sub>2</sub> SO <sub>4</sub>	AR	10 vol.-%

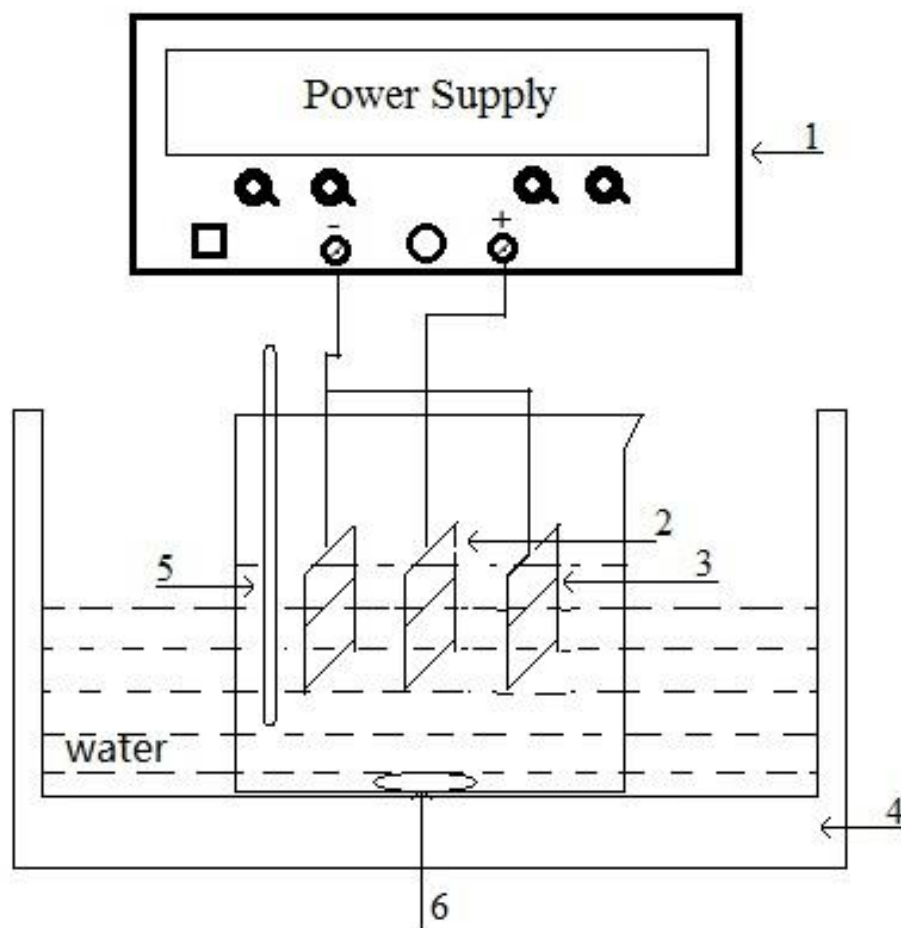


**Figure 1.** Anodic oxidation experiment equipment:(1)power supply;(2)sample;(3)titanium sheet cathode;(4)thermostatic water bath;(5)thermometer;(6)stirrer

The anodized samples were put into SBF with the volume of 25mL for 7d for biological activity tests. The SBF was composed of  $\text{Na}^+$  142,  $\text{K}^+$  5.0,  $\text{Mg}^{2+}$  1.5,  $\text{Ca}^{2+}$  2.5,  $\text{Cl}^-$  147.8,  $\text{HCO}_3^{-}$  4.2,  $\text{HPO}_4^{2-}$  1.0, and  $\text{SO}_4^{2-}$  0.5 mM, which was near human blood plasma. In addition, the pH of SBF were adjusted to 7.45 at 37°C.

The anticorrosion tests were carried out in Hank's simulated physiologic solution[32] under the conditions of the pH=7.45 and t=37°C through PARSTAT 2273 compatible with PowerSuite software. The Hank's simulated physiologic solution was prepared by sodium chloride(NaCl) 8, potassium chloride (KCl) 0.4, sodium bicarbonate ( $\text{NaHCO}_3$ ) 0.35, potassium dihydrogen phosphate ( $\text{KH}_2\text{PO}_4$ ) 0.06, anhydrous calcium chloride ( $\text{CaCl}_2$ ) 0.14, magnesium chloride hexahydrate ( $\text{MgCl}_2 \cdot 6\text{H}_2\text{O}$ ) 0.1, magnesium sulfate heptahydrate ( $\text{MgSO}_4 \cdot 7\text{H}_2\text{O}$ ) 0.06, twelve-hydrated disodium hydrogen phosphate ( $\text{Na}_2\text{HPO}_4 \cdot 12\text{H}_2\text{O}$ ) 0.1 and glucose 1 g/L, which was near human blood plasma. Cyclic polarization measurement was made through three-electrode system. The anodized TA2 titanium alloy with working areas of  $0.5 \times 0.5\text{cm}^2$  was used as the working electrode, which the reference electrode and counter electrode were saturated calomel electrode (SCE) and platinum plate in the process of the cyclic polarization. The cyclic scan started from -1.0V (vs OCP) to 6.0V ( $E_{sw}$ , vs OCP). The potential scan rate was 1mV/s.

The scanning electron microscopy (SEM: HITACHI SU 8010) and X-ray diffraction (XRD: D2 PHASER) were used for measuring microstructure of the anodized TA2 titanium, after soaking in SBF. The atomic ratios on the surface after soaking were analysed by EDS.

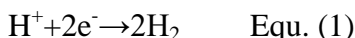
### 3. RESULTS AND DISCUSSION

#### 3.1 The formation of porous film

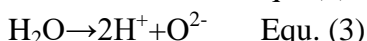
In the initial stage of anodic oxidation, compact film(barrier layer) formed on the TA2 titanium surface due to the larger current density; with the rapid decrease of the current density, microscopic fluctuation on the surface of the substrate would cause that current density distributed unevenly on the barrier layer, and electric field would focus on depression of anodized surface, so that the dissolution rate of depression increased, finally resulting in the porous structure.

Chemical equation of titanium anodized layers' formation:

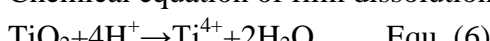
cathode reaction:



anode reaction:

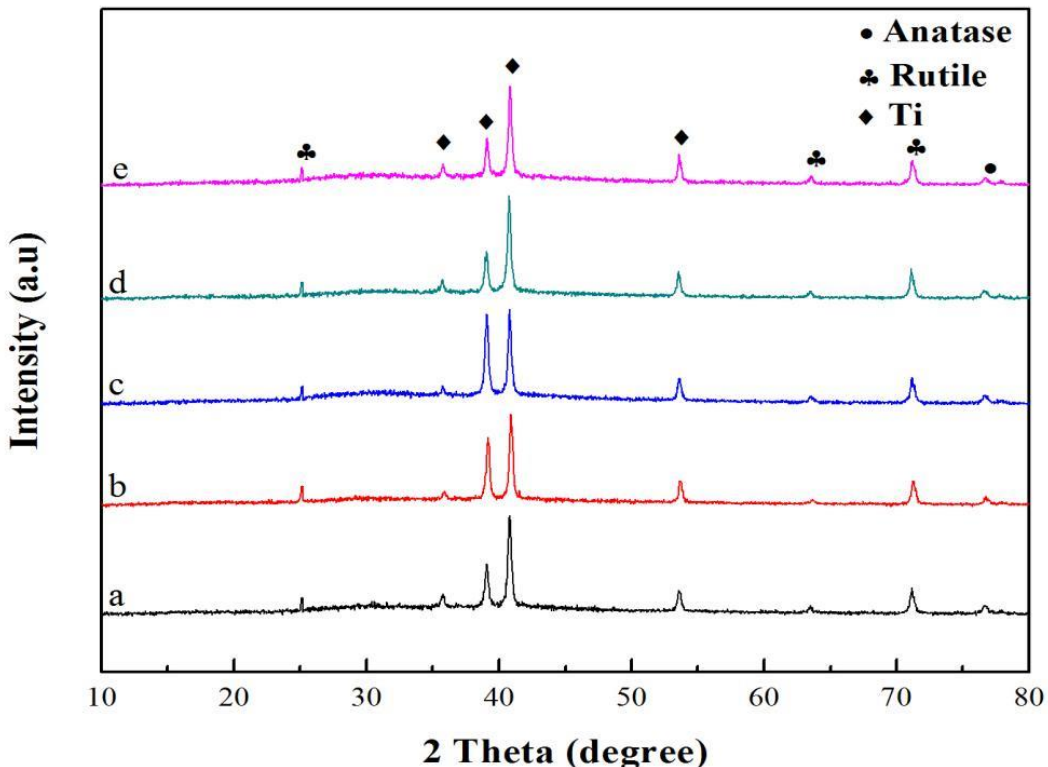


Chemical equation of film dissolution:



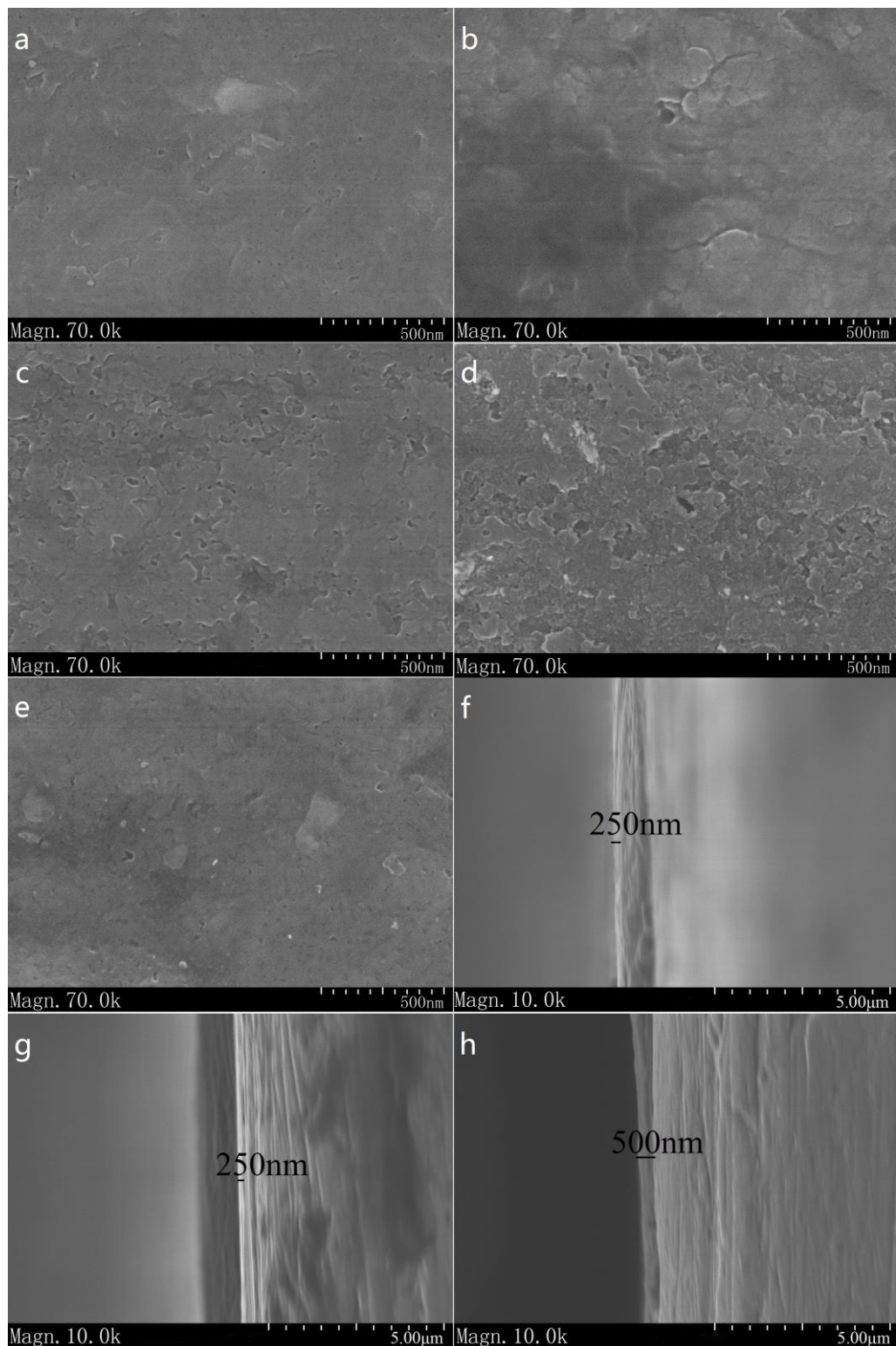
### 3.2 Effects of anodized voltage on the microstructures of TA2

Figure 2 showed the XRD patterns of TA2 titanium alloy anodized under the condition of different voltages. Rutile and anatase titania formed on the anodized TA2 titanium alloy surface.



**Figure 2.** XRD patterns of TA2 anodized at different voltages: (a) 10V; (b) 20V; (c) 30V; (d) 40V; (e) 50V. Samples were anodized in the electrolyte exhibited in Tab.1 at 25°C for 20 min.

The peaks of rutile and anatase titania were weaker, the other peaks of TA2 were stronger, and the peaks of Ti did not change with voltages increasing which may because the anodized voltage was low. According to Yang et al.[27], the titanium metals was anodized at 90V, 155V and 180V, found that the peaks of Ti decreases with the voltage increasing, and disappeared when anodized 180V. Figure 3 showed that the SEM morphology of anodized TA2 titanium alloy. The surface existed porous structures. The porosities and roughness of the anodized films increased with the anodized voltages increasing. The thickness of the layer achieved about 500nm, when anodized under DC 30V showed in Figure 3(h), while which was 250nm anodized at DC 10V and 20V. However, when the applied voltage continued to increase, the thickness of the anodized layers maintained about 500 nm and the thickness had not been shown in this figure.



**Figure 3.** SEM micrograph of TA2 titanium alloy anodically oxidized at different voltages: (a) 10V; (b) 20V; (c) 30V; (d) 40V; (e) 50V; (f) 10V for cross-sectional morphology; (g) 20V for cross-sectional morphology; (h) 30V for cross-sectional morphology. Samples were anodized in the electrolyte exhibited in Tab.1 at 25°C for 20 min.

### 3.2.1 Apatite formation of anodized TA2 titanium under the condition of different voltages

Anodized TA2 titanium alloy with the area of  $1 \times 1\text{cm}^2$  was cleaned in deionized water and dried by hair dryer. One of the side sealed by adhesive tape and another side was soaking with no tape. The prepared anodized TA2 titanium was soaked in SBF for 7d at  $37^\circ\text{C}$ . The SBF was changed every day.

Apatite formed on the surface of TA2 titanium anodized at various voltages when they were soaked in the SBF for 7d (Figure 4). Some of them presented spherical, and others presented sheet appearance, which may be due to the different roughness of the surfaces. As discussed in Wei [33], the larger surface roughness, the more formation of active sites when soaking in the simulated body fluids. Apatite nucleation was widely distributed, aggregation phenomenon was not obvious, the average particle size of the formed apatite polycrystalline nuclei was small. The roughness of the surfaces related certainly to the polished in pre-treated process. What's more, different areas of the same titanium alloy plate and apatite layer depositions were also different. When anodized at DC 10V, 40V and 50V, obviously, different sizes of spherical apatite formed. Some were petals shapes (figure 4d), and others were nubbly (Figure 4a.e). The apatite layers were flaky anodized at DC 20V and 30V (Figure 4b.c). The apatite covered most parts of the surface anodized at DC 40V which means there was a higher period of apatite formation under this circumstance. Table 2 showed that the atomic ratio (Ca/P) of TA2 titanium alloys soaked in SBF for 7d after they were anodically oxidized at different voltage which measured by EDS. The atomic ratio of Ca/P achieved 1.27 anodised at DC 40V, compared with the ideal atomic ratio of Ca/P of hydroxyapatite (1.67). It was short of calcium. As discussed in Ref,[34] the surface chemistry of the titanium substrates played an important role in inducing apatite formation.

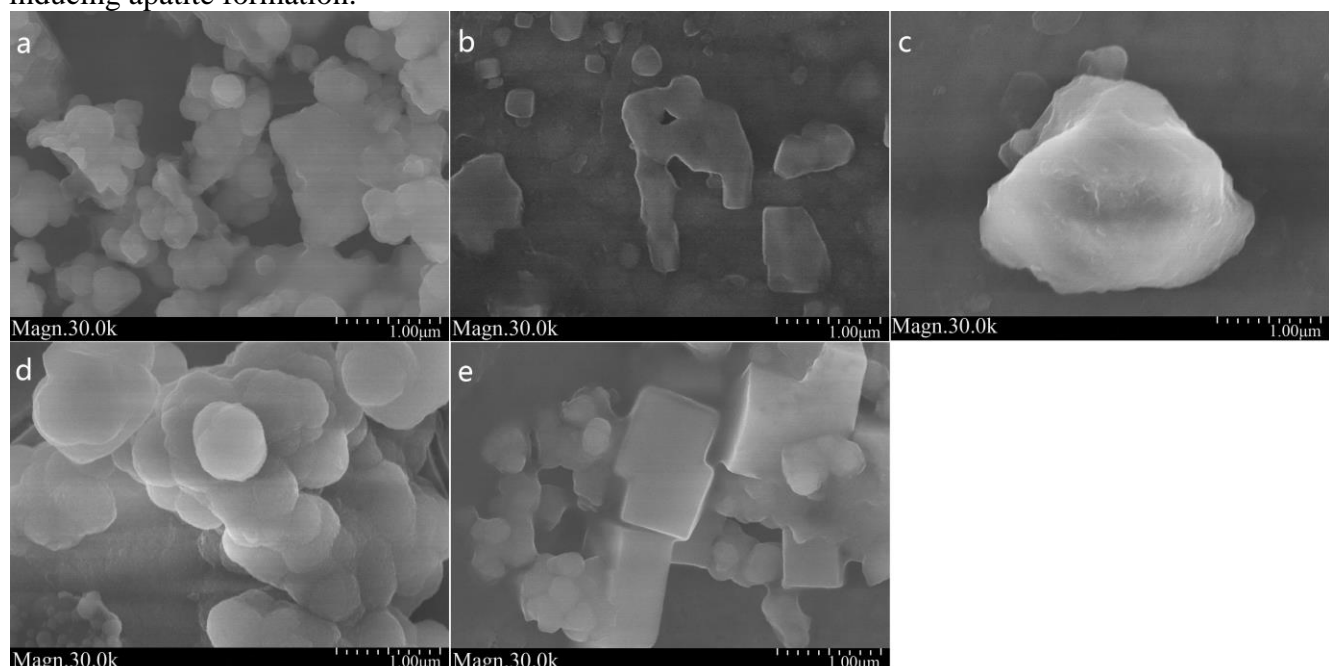


**Figure 4.** Surface morphology of samples soaked in SBF for 7d after they were anodically oxidized at different voltages:(a)10V;(b)20V;(c)30V;(d)40V;(e)50V. Samples were anodized in the electrolyte exhibited in Tab.1 at  $25^\circ\text{C}$  for 20 min.

**Table 2.** Ca/P of samples soaked in SBF for 7d after they were anodically oxidized at different voltages

Voltage(V)	Ca/P
10	0.90
20	0.88
30	0.80
40	1.27
50	0.90

### 3.2.2 Corrosion resistance of anodised TA2 titanium alloy films under different voltages

For the sake of stability as well as corrosion resistance of the implant materials in the human body environment, it was necessary to conduct circular polarization test in Hank's solution nearly human blood plasma.

Cyclic polarization measurements which revealed that the chronic corrosion behavior would take place under human environment[1], forced the material from its steady state by sweeping the potential in the anodic direction and stopped at predetermined switching potential ( $E_{sw}$ ). Then the polarization continued in the cathodic direction in reverse. Among them, the switching potential was 6.0V,  $E_{corr}$  and  $E'_{corr}$  represented the corrosion potential of the first polarized and returned.

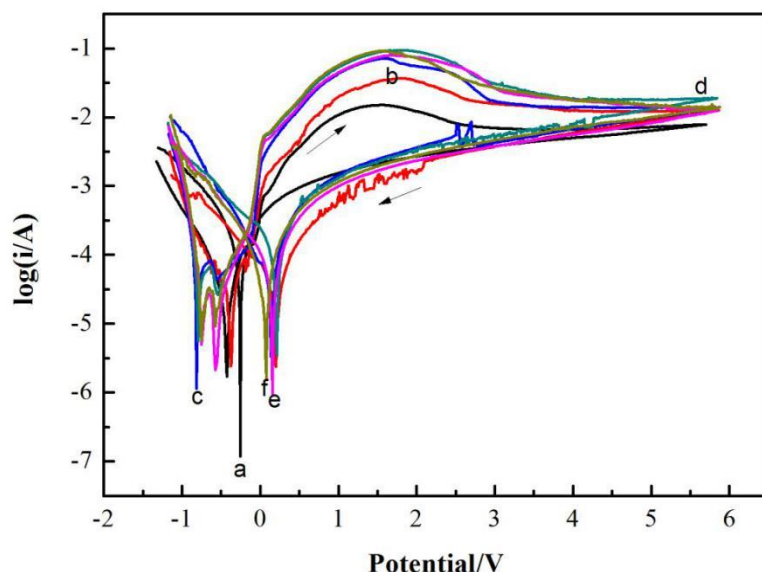


**Figure 5.** Cyclic polarization curves measured in Hank's solution (pH 7.45,  $t=37^\circ\text{C}$ ) anodically oxidized at different voltages:(a)TA2; (b)10V; (c)20V; (d)30V; (e)40V; (f)50V. Samples were anodized in the electrolyte exhibited in Tab.1 at  $25^\circ\text{C}$  for 20 min.

**Table 3.** Corrosion parameters measured in Hank's solution (pH 7.45, t=37°C) anodically oxidized at different voltage;  $\Delta E = (E_{sw} - E_{corr})$  and  $\Delta E' = (E'_{sw} - E'_{corr})$ 

Voltage(V)	$E_{corr}(V)$	$i_{corr}(A/cm^2)$	$E'_{corr}(V)$	$\Delta E(V)$	$\Delta E'(V)$
Untreated	-0.422	$2.725 \times 10^{-4}$	-0.252	6.422	6.252
10	-0.376	$6.160 \times 10^{-5}$	0.204	6.376	5.796
20	-0.811	$8.617 \times 10^{-5}$	0.139	6.811	5.861
30	-0.797	$5.119 \times 10^{-5}$	0.213	6.797	5.787
40	-0.572	$2.044 \times 10^{-5}$	0.158	6.572	5.842
50	-0.752	$4.846 \times 10^{-5}$	0.078	6.752	5.922

The cyclic polarization curves for TA2 measured in Hank's solution anodically oxidized at different voltage and untreated were presented in Figure 5, and the corresponding corrosion parameters were also presented in Table 3. It could be observed that the corrosion current density of anodised TA2 titanium alloy decreased a magnitude which demonstrated the anticorrosion improved. With the oxidation voltage increasing, the corrosion current density were the same magnitude, but the values were different, that took the minimum ( $2.044 \times 10^{-5} A/cm^2$ ) when anodically oxidized at DC 40V. The corrosion resistance achieved the best while the oxidation voltage was DC 40V. The values of  $\Delta E$  and  $\Delta E'$  indicated that the stability of the films in the cyclic polarization scanning process, and the larger the values, the better the stability; which discussed in detail in research of Cotolan et. al[1]. It could be see that anodizing at different voltage for TA2 was not obvious for stability improvement in the scanning process.

### 3.3 Effects of oxidation duration on the microstructures of the films

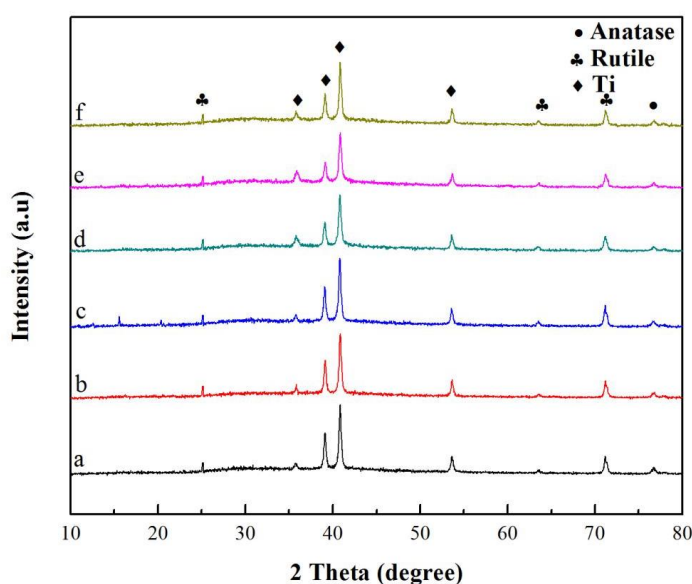
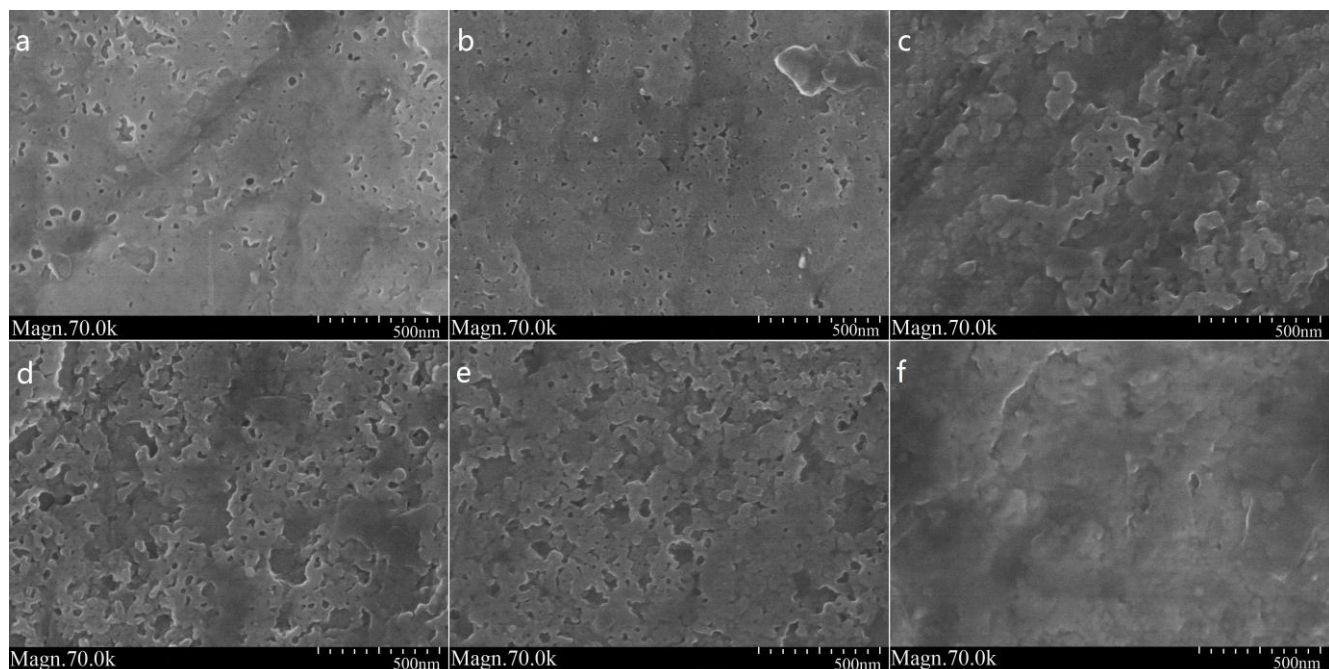
**Figure 6.** XRD patterns of TA2 titanium alloy anodically oxidized for different oxidation durations: (a)10min; (b)20min; (c)30min; (d)40min; (e)50min; (f)60min. Samples were anodized in the electrolyte exhibited in Tab.1 under 30 V at 25°C..

Figure 6 revealed the XRD patterns of TA2 titanium alloy anodically oxidized at different anodized durations.



**Figure 7.** Surface morphologies of TA2 titanium alloy anodically oxidized for different oxidation durations:(a)10min;(b)20min;(c)30min;(d)40min;(e)50min;(f)60min. Samples were anodized in the electrolyte exhibited in Tab.1 under 30 V at 25°C.

Rutile and anatase titania, whose the peaks were weaker, appeared on the surface after the anodization; and the peaks of Ti did not change with voltages increasing; which was the same as Figure 2. Figure 7 showed that SEM photos of TA2 titanium alloy after the anodization. The oxide films were typically porous membranes which was similar with the films anodized at high voltages[27]. With the oxidation duration increasing, the surfaces with more porosities performed rougher. However, while the TA2 titanium alloy anodically oxidized for 60 min, hardly any porosity was observed on the surface.

### 3.3.1 Apatite formation of anodised TA2 titanium alloy film for different oxidation durations

The soaking test in SBF for 7d was on the same as 3.1.1. Apatite formed on the TA2 titanium alloy anodised for 10-40min when they were soaked in the SBF for 7d (Figure 8a.b.c.d), while hardly any apatite formation was on the films anodised for 50min and 60min (Figure 8e.f). It could be observed that there was a higher period of apatite formation when anodised for 10min and 40min, and most regions of the films anodically oxidized for 50min and 60min were eroded by SBF and peeled off, which resulted in bare substrates and caused substrates eroded[33]. Table 4 showed that the atomic ratio (Ca/P) of TA2 titanium alloys soaked in SBF for 7d after they were anodically oxidized for

different oxidation durations which measured by EDS. The atomic ratios of Ca/P were mainly about 0.9, compared with the ideal atomic ratio of Ca/P of hydroxyapatite (1.67), it was short of calcium. It might due to the surface chemistry of the substrates[34].

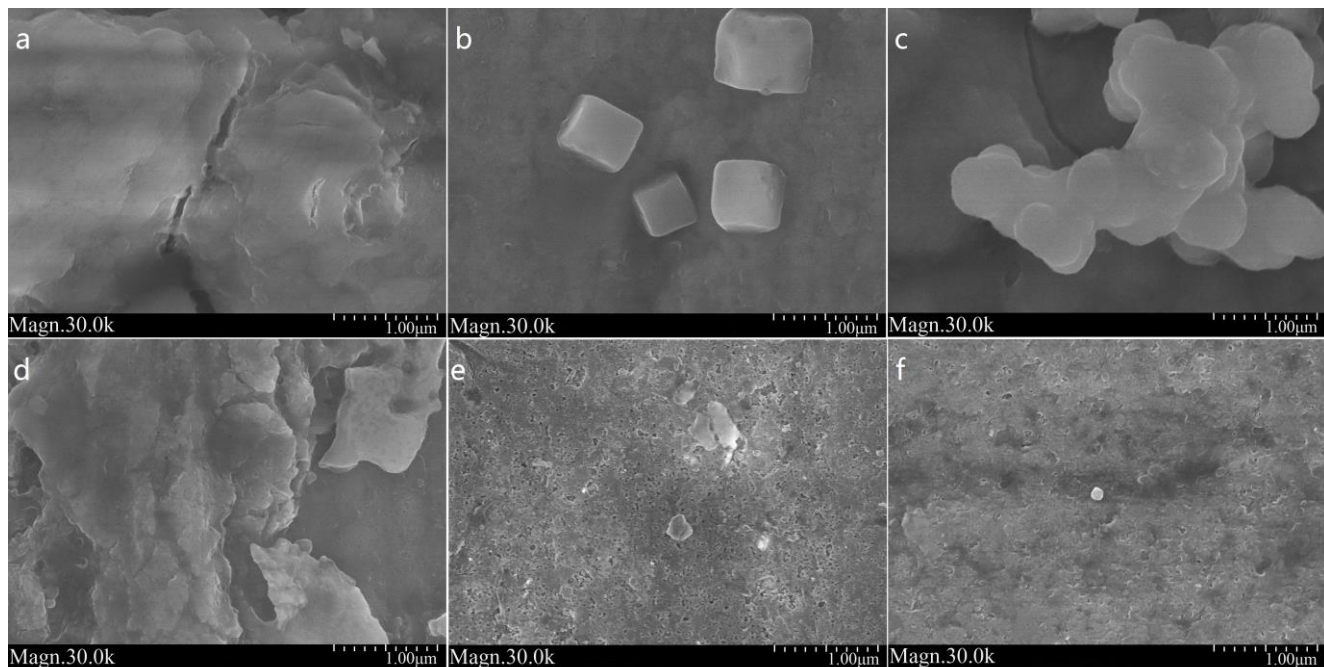


**Figure 8.** Surface morphology of samples soaked in SBF for 7d after they were anodically oxidized for different oxidation times:(a)10min;(b)20min;(c)30min;(d)40min;(e)50min;(f)60min. Samples were anodized in the electrolyte exhibited in Tab.1 under 30 V at 25 °C.

**Table 4.** Ca/P of samples soaked in SBF for 7d after they were anodically oxidized for different oxidation times

oxidation time(min)	Ca/P
10	0.91
20	0.90
30	0.90
40	0.91
50	0.89
60	0.90

### 3.3.2 Corrosion resistance of anodised TA2 titanium alloy films for different oxidation durations

Cyclic polarization measured on the same with 3.1.2. The cyclic polarization curves for TA2 measured in Hank's solution anodically oxidized for different oxidation durations were presented in Figure 9, and the corresponding corrosion parameters were also presented in Table 5.

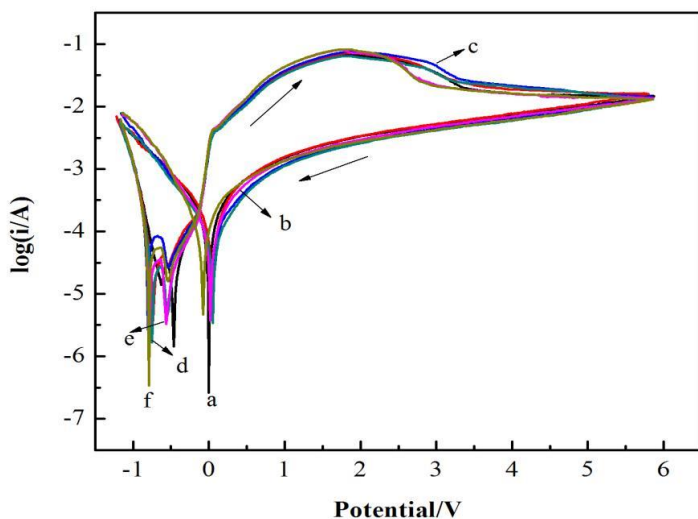


**Figure 9.** Cyclic polarization curves measured in Hank's solution ( $\text{pH } 7.45$ ,  $t=37^\circ\text{C}$ ) anodically oxidized for different durations:(a)10min;(b)20min;(c)30min;(d)40min;(e)50min;(f)60min. Samples were anodized in the electrolyte exhibited in Tab.1 under 30 V at  $25^\circ\text{C}$ .

**Table 5.** Corrosion parameters measured in Hank's solution ( $\text{pH } 7.45$ ,  $t=37^\circ\text{C}$ ) anodically oxidized for different durations;  $\Delta E=(E_{\text{sw}}-E_{\text{corr}})$  and  $\Delta E'=(E'_{\text{sw}}-E'_{\text{corr}})$

Time(min)	$E_{\text{corr}}(\text{V})$	$i_{\text{corr}}(\text{A}/\text{cm}^2)$	$E'_{\text{corr}}(\text{V})$	$\Delta E(\text{V})$	$\Delta E'(\text{V})$
10	-0.461	$4.842 \times 10^{-5}$	-0.000757	6.461	6.000757
20	-0.740	$7.728 \times 10^{-5}$	0.0500	6.740	5.9500
30	-0.809	$9.103 \times 10^{-5}$	0.0415	6.809	5.9585
40	-0.751	$2.725 \times 10^{-5}$	0.0488	6.751	5.9512
50	-0.782	$5.558 \times 10^{-5}$	0.0177	6.782	5.9823
60	-0.794	$7.113 \times 10^{-5}$	-0.0736	6.794	6.0736

The corrosion current density of anodised TA2 titanium alloy decreased a magnitude compared with untreated TA2 titanium which demonstrated the anticorrosion improved (Table 4). With the oxidation duration increasing, the corrosion current density were the same magnitude, but the values were different, that took the minimum ( $2.725 \times 10^{-5} \text{ A/cm}^2$ ) when anodically oxidized for 40min. It meant the corrosion resistance achieved the best while anodised for 40min. The values of  $\Delta E$  and  $\Delta E'$  indicated that the stability of the films in the cyclic polarization scanning process, and the larger the values, the better the stability[1]. It could be also seen that anodizing for different oxidation durations for TA2 titanium was not obvious for stability improvement in the scanning process.

#### 4. CONCLUSIONS

In summary, porous anatase and rutile has been fabricated on the TA2 titanium alloy surface via anodic oxidation. The porosities of the anodized films increased with the anodized voltages and

oxidation durations increasing. The thickness of the oxide layer achieved about 500nm. After anodizing, experimental results exhibited that the corrosion resistance has been largely improved, due to that the corrosion current density ( $2.044 \times 10^{-5} \text{ A/cm}^2$  and  $2.725 \times 10^{-5} \text{ A/cm}^2$ ) decreased a magnitude compared with untreated TA2 titanium ( $2.725 \times 10^{-4} \text{ A/cm}^2$ ), when the TA2 titanium was anodized under the condition of DC 40V for 40 min. After soaking in SBF, apatite formed on the  $\text{TiO}_2$  layers grown with different shapes and it covered most parts of the surface when anodized at DC 40V for 10min. In addition, the atomic ratio (Ca/P) of the apatite films which demonstrated that the films were short of calcium compared to hydroxyapatite.

#### ACKNOWLEDGEMENT

This research was supported by the National Natural Science Foundation (No. 51471156) and International Science and Technology cooperation Program of China (No. 2011DFA52400).

#### References

1. N. Cotolan, A. Pop, D. Marconi, O. Ponta and L. M. Muresan, *Mater. Corros.*, 66 (2015) 635.
2. M. L. Vera, E. Linardi, L. Lanzani, C. Mendez, C. E. Schvezov and A. E. Ares, *Mater. Corros.*, 66 (2014) 1.
3. I. Gligor, O. Soritau, M. Todea, C. Berce, A. Vulpoi, T. Marcu, V. Cernea, S. Simon and C. Popa, *Part. Sci. Technol. An Int. J.*, 31 (2013) 357.
4. M. Niinomi, *Biomaterials*, 24 (2003) 2673.
5. L. F. Zhuang, H. H. Jiang, S. C. Qiao, C. Appert, M. S. Si, Y. S. Gu and H. C. Lai, *J. Biomed. Mater. Res.*, 100 (2012) 125.
6. J. R. S. Martins Júnior, R. A. Nogueira, R. O. de Araújo, T. A. G. Donato, V. E. Arana-Chavez, A. P. R. A. Claro, J. C. S. Moraes, M. A. R. Buzalaf and C. R. Grandini, *Mater. Res.*, 14 (2011) 107.
7. S. Bodhak, S. Bose and A. Bandyopadhyay, *Acta Biomater.*, 5 (2009) 2178.
8. D. N. Heo, W. K. Ko, H. R. Lee, S. J. Lee, D. Lee, S. H. Um, J. H. Lee, Y. H. Woo, L. G. Zhang and W. D. Lee, *J. Colloid. Interf. Sci.*, 469 (2016) 129.
9. M. Geetha, A. K. Singh, R. Asokamani and A. K. Gogia, *Prog. Mater. Sci.*, 54 (2009) 397.
10. N. J. Hallab, S. Anderson, T. Stafford, T. Glant and J. J. Jacobs, *J. of Orthop. Res.*, 23 (2005) 384.
11. S. A. Fadlallah and Q. Mohsen, *Appl. Surf. Sci.*, 256 (2010) 5849.
12. H. T. Chen, C. J. Chung, T. C. Yang, C. H. Tang and J. L. He, *Appl. Surf. Sci.*, 266 (2013) 73.
13. M. P. Casaletto, G. M. Ingo, S. Kaciulis, G. Mattogno, L. Pandolfi and G. Scavia, *Appl. Surf. Sci.*, 172 (2001) 167.
14. V. Piazza, A. Mazare, M. V. Diamanti, M. P. Pedeferri and P. Schmuki, *J. Elecrochem. Soc.*, 163 (2016) H119.
15. Y. L. Chung, D. S. Gan and K. L. Ou, *J. Elecrochem. Soc.*, 159 (2012) C133.
16. H. T. Chen, H. Y. Shu, C. J. Chung and J. L. He, *Surf. Coat. Technol.*, 276 (2015) 168.
17. S. A. Yavari, J. V. D. Stok, Y. C. Chai, R. Wauthle, Z. T. Birgani, P. Habibovic, M. Mulier, J. Schrooten, H. Weinans and A. A. Zadpoor, *Biomaterials*, 35 (2014) 6172.
18. S. A. Yavari, Y. C. Chai, A. J. Bottger, R. Wauthle, J. Schrooten, H. Weinans and A. A. Zadpoor, *Mater. Sci. Eng.*, C, 51 (2015) 132.
19. D. Kakoli, B. Susmita and B. Amit, *J. Biomed. Mater. Res. Part A*, 90 (2009) 225.
20. S. Minagar, C. C. Berndt, J. Wang, E. Ivanova and C. Wen, *Acta Biomater.*, 8 (2012) 2875.
21. B. E. Li, Y. Li, J. Li, X. L. Fu, H. P. Li, H. S. Wang, S. G. Xin, L. X. Zhou, C. Y. Liang and C. Y.

- Li, *J. Mater. Sci.-Mater. Med.*, 25 (2014) 199.
22. H. H. Huang, C. P. Wu, Y. S. Sun, H. M. Huang and T. H. Lee, *Thin Solid Films*, 549 (2013) 87.
23. B. E. Li, Y. Li, J. Li, X. L. Fu, C. Y. Li, H. S. Wang, S. M. Liu, L. T. Guo, S. G. Xin, C. Y. Liang and H. P. Li, *Appl. Surf. Sci.*, 307 (2014) 202.
24. Z. Ozdemir, A. Ozdemir and G. B. Basima, *Mater. Sci. Eng., C-Mater.*, 68 (2016) 383.
25. D. Babilas, E. Urbanczyk, M. Sowa, A. Maciej, D.M. Korotin, I.S. Zhidkov, M. Basiaga, M. Krok-Borkowicz, L. Szyk-Warszynska, E. Pamula, E.Z. Kurmaev, S.O. Cholakh and W. Simka, *Electrochim. Acta*, 205 (2016) 256.
26. H. Habazaki, K. Shimizu, S. Nagata, P. Skeldon, G. E. Thompson, G. C. Wood, *Corros. Sci.*, 44 (2002) 1047.
27. B. C. Yang, M. Uchidab, H. M. Kim, X. D. Zhang and T. Kokubo, *Biomaterials*, 25, (2004) 1003.
28. H. C. Hsu, S. C. Wu, S. K. Hsu, Y. C. Chang and W. F. Ho, *Mater. Charact.*, 100 (2015) 170.
29. K. Lee, H. C. Choe, B. H. Kim and Y. M. Ko, *Surf. Coat. Technol.*, 205 (2010) S267.
30. C. X. Yue and B. C. Yang, *J. Bionic Eng.*, 11 (2014) 589.
31. A. A. Zadpoor, *Mater. Sci. Eng., C-Mater.*, 35 (2014) 134.
32. Z. Q. Mou and C. H. Liang, *J. Chin. Soc. Corros. Prot.*, 18 (1998) 126.
33. C. L. Wei, *Funct. Mater.*, 2 (2011) 516.
34. K. Suchanek, A. Bartkowiak, A. Gdowik, M. Perzanowski, S. Kac, B. Szaraniec, M. Suchanek and M. Marszalek, *Mater. Sci. Eng., C-Mater.*, 51 (2015) 57.

© 2017 The Authors. Published by ESG ([www.electrochemsci.org](http://www.electrochemsci.org)). This article is an open access article distributed under the terms and conditions of the Creative Commons Attribution license (<http://creativecommons.org/licenses/by/4.0/>).